

SCIENTIFIC REPORTS



OPEN

A highly diverse, desert-like microbial biocenosis on solar panels in a Mediterranean city

Received: 04 January 2016

Accepted: 13 June 2016

Published: 05 July 2016

Pedro Dorado-Morales^{1,*}, Cristina Vilanova^{1,2,*}, Juli Peretó^{1,2,3,†}, Francisco M. Codoñer⁴, Daniel Ramón⁵ & Manuel Porcar^{1,2,†}

Microorganisms colonize a wide range of natural and artificial environments although there are hardly any data on the microbial ecology of one of the most widespread man-made extreme structures: solar panels. Here we show that solar panels in a Mediterranean city (Valencia, Spain) harbor a highly diverse microbial community with more than 500 different species per panel, most of which belong to drought-, heat- and radiation-adapted bacterial genera, and sun-irradiation adapted epiphytic fungi. The taxonomic and functional profiles of this microbial community and the characterization of selected culturable bacteria reveal the existence of a diverse mesophilic microbial community on the panels' surface. This biocenosis proved to be more similar to the ones inhabiting deserts than to any human or urban microbial ecosystem. This unique microbial community shows different day/night proteomic profiles; it is dominated by reddish pigment- and sphingolipid-producers, and is adapted to withstand circadian cycles of high temperatures, desiccation and solar radiation.

Today, photovoltaic panels cover around 4000 square kilometers, and are forecasted to be the world's main electricity source by 2050 (<http://www.epia.org>). Solar panels are unique biotopes characterized by a smooth flat glass or glass-like surface, minimum water retention capacity and maximum sunlight exposure, all of which determine circadian and annual peaks of irradiation, desiccation and heat. Extreme natural habitats such as thermal vents, mountain plateaus or hyper arid deserts are known to host microbial biocenoses adapted to those particular selection pressures^{1–3}; and artificial or humanized environments, such as industrial reactors⁴, radioactive waste⁵ or oil spills⁶ are also colonizable by specialized microorganisms. Among artificial environments, indoor biomes constitute around 0.5% of the ice-free land area, a surface comparable to the subtropical coniferous forest⁷. Geography and building type, among other factors, structure indoor microbes, which are inoculated by human skin and outdoor air⁸ and even by indoor plants⁹. One of the recently studied indoor habitats is the subway. A recent study of the aerosol microbial communities of the New York City subway platforms¹⁰ revealed that such communities were a mixture of soil, environmental water, and human skin commensal bacteria. In a similar work in the Hong Kong subway networks¹¹, researchers found that each subway line harbored a different phylogenetic community, depending on architectural characteristics, nearby (outdoor) microbiomes, as well as connectedness with other lines.

Most of the so-called built environment studies have so far focused in the indoor biomes but less attention has been paid to artificial, outdoor environments. A recent example of those is an ambitious city-scale metagenomics screening on the bacterial diversity of New York (including both indoor and outdoor biomes), which found a very high diversity of microorganisms -roughly 1700 bacterial taxa-, half of which did not match any known organism¹². However, many artificial outdoor environments remains unexplored to date.

In the present work, we aimed at studying solar panels, an outdoor artificial environment whose role as biotope had not previously been reported. The goal of our study was to identify possible microbial communities thriving in the harsh conditions of the panels' surfaces, and to determine to which extent this highly irradiated

¹Institut Cavanilles de Biodiversitat i Biologia Evolutiva, Universitat de València, Paterna 46980, Spain. ²Darwin Bioprospecting Excellence, S.L., Parc Científic Universitat de València, Paterna, Valencia, Spain. ³Departament de Bioquímica i Biologia Molecular, Universitat de València, Burjassot 46100, Spain. ⁴Lifesequencing S.L., Parc Científic Universitat de València, Paterna, Spain. ⁵Biopolis S.L., Parc Científic Universitat de València, Paterna, Valencia, Spain. [†]Present address: Institute for Integrative Systems Biology (I2SysBio, Universitat de València-CSIC), Parc Científic Universitat de València, Paterna, Valencia, Spain. *These authors contributed equally to this work. Correspondence and requests for materials should be addressed to M.P. (email: manuel.porcar@uv.es)

environment was home of ecologically extremophile bacteria (thermophilic and radio-resistant taxa, for example), as well as to identify microbial strains with biotechnological applications, such as carotenoid producers.

Our report documents a complete bioprospection and characterization of the microbial community on photovoltaic panels of a Mediterranean city, using high throughput 16S/18S rRNA analysis, metagenomic sequencing, metaproteomics, and culture-based characterization of selected isolates.

Results

Culturing of solar panel samples from the 2013 solstice on LB, R2A, and marine media yielded a relatively high number of colony forming microorganisms, mostly bacteria, displaying a wide range of color and shapes. Many of the isolates displayed red, orange or pink pigmentation (Figure S1), particularly those incubated on marine agar. A total of 53 pigmented isolates were selected and subjected to taxonomic (16S rRNA) characterization and tested for resistance to heat (incubation at 60 °C), UV exposure (2 to 30 s pulses of a 340 $\mu\text{W cm}^{-2}$ UV light), high NaCl contents (1 to 26%) and different pH values (5 to 9). Most of the solar-panel isolates displayed resistance to very high salt concentrations (20–26% w/v NaCl) and short exposures to UV light, whereas only a few number of isolates proved resistant to a low pH or extreme heat (Figure S2). Interestingly, during these characterization assays we were able to identify isolates able to restore the growth of nearby isolates under conditions of extreme salt or pH values, in the latter case because of local buffering of the pH of the plate (Figure S1). Full characterization of the 53 isolates is provided in Table S1 and Figure S2.

The taxonomic composition of bacterial and eukaryotic taxa was first studied through 16S and 18S rRNA genes massive sequencing; the results are shown in Fig. 1. As many as 800 different bacterial species were identified in the 2013 pool (nine solar panels from different locations within the University of Valencia); and around 500 different species were found in each of the individual panels sampled from a single building in 2014 (Table S2). Two orders, Sphingobacteriales (families Flexibacteriaceae and Sphingomonadaceae) and Deinococcales comprised the highest number of species. *Deinococcus*, *Sphingomonas*, *Novosphingobium* or *Hymenobacter* were the dominant genera, with 9.2% or 28% of the assigned sequences (*H. chitinivorans* in panel 1 and *D. hopiensis* in panel 3, respectively). The remaining sequences were distributed among 17 phyla and 146 families. Other well-represented genera, in order of abundance, were *Rubellimicrobium*, *Adhaeribacter*, *Acidicaldus*, *Segetibacter*, or *Modestobacter*. In the case of fungi, lower biodiversity was found (Fig. 1B). Taxonomic eukaryotic profiles were dominated by the phylum Ascomycota and the families Pleosporaceae and Teratosphaeriaceae, with genera *Phaeothecoidea* and *Alternaria* representing the majority in the 2013 and 2014 samples, respectively.

In 2014, the metagenomic DNA of two independent solar panels was shotgun sequenced. As shown in Fig. 1C, the ratio of bacteria:fungi reads was close to 50%, and species distribution was similar to that found for 16S and 18S rRNA sequencing. Genus *Deinococcus*, one of the clearest taxonomic markers of extremophily, again proved highly abundant in all our samples. A summary of sequencing statistics and diversity indexes can be accessed in Table S3. The core microbiome, understood as the number of species detected in all the samples analyzed, comprised around 120 species (26% of the total number of species detected), and was composed, mainly, by members of the *Deinococcus*, *Sphingomonas*, *Novosphingobium*, and *Hymenobacter* genera.

We analyzed *Deinococcus* sequences from our metagenomic analysis and a draft *Deinococcus* solar panel pangenome of 2098 contigs was obtained, covering more than 0,8 Mb (25%) of standard *Deinococcus* genomes (3.3Mb with 2 chromosomes and 2 plasmids), with 2166 and 149 ORFs and tRNAs, respectively (Fig. 1D). The low identity level of the solar panel pangenome with previously sequenced *Deinococcus* species strongly suggests that at least one previously undescribed *Deinococcus* species is present in the sampled panels.

Regarding the functional profile, that of two independent solar panels (1 and 3) was deduced from the metagenomic data, and statistically analyzed with the STAMP software. When compared to a range of metagenomes from diverse habitats, solar-panel functional profiles clustered together with those described for polar microbial mat and saline desert datasets, and distant to those of other environments such as air or sediments (Fig. 2A). Both solar panels proved very similar to each other in terms of functions, as shown in Fig. 2B. The bioactivity of the biocenosis was studied through a metaproteomic analysis conducted on solar panels sampled at noon (solar time) and at night (4 AM). Protein composition differed between the day and night samples (Fig. 2C). Significantly, a protein involved in modulating bacterial growth on surfaces and biofilm formation¹³ (diguanylate cyclase) was particularly abundant. Also among the more expressed proteins, we identified fungal and bacterial enzymes involved in respiration and ATP synthesis or ribosomal proteins (bacterial L7/L12 and archaeal L7, the latter being a moonlighting protein involved in rRNA processing¹⁴). Other abundant proteins have been reported to confer resistance/tolerance to the extreme conditions found in solar panels, namely, salt stress and drought (membrane-bound proton-translocating pyrophosphatase mPP¹⁵), nutrient starvation (mPP and cold-shock protein¹⁶), heat-shock (molecular chaperone GroEL), as well as proteins involved in the preservation of membrane integrity under harsh conditions^{17,18} (S-layer protein, lipoprotein 1; Table S4).

Discussion

Despite the harsh conditions to which microorganisms deposited -or permanently inhabiting- the solar panels of a Mediterranean city are subjected during summer, standard culturing resulted in important microbial growth, with a diversity in shape, color and textures of colony forming microorganisms from the 2013 solstice suggesting high biodiversity of the environment. Although culturable isolates are typically only a small fraction of the global biocenosis, we were able to identify several strain-to-strain effects that proved able to restore the sensitivity of neighboring isolates to stress factors (salinity and low pH). These results suggest that microbial interactions and the particular physical location of microorganisms on the solar panels, rather than individual cell properties, might play a major role in bacterial survival on solar panels.

High throughput sequencing allowed confirming the high diversity of the habitat in the form of a sun-adapted taxonomic profile. Indeed, and in accordance with the majoritary phenotype observed within culturable isolates,

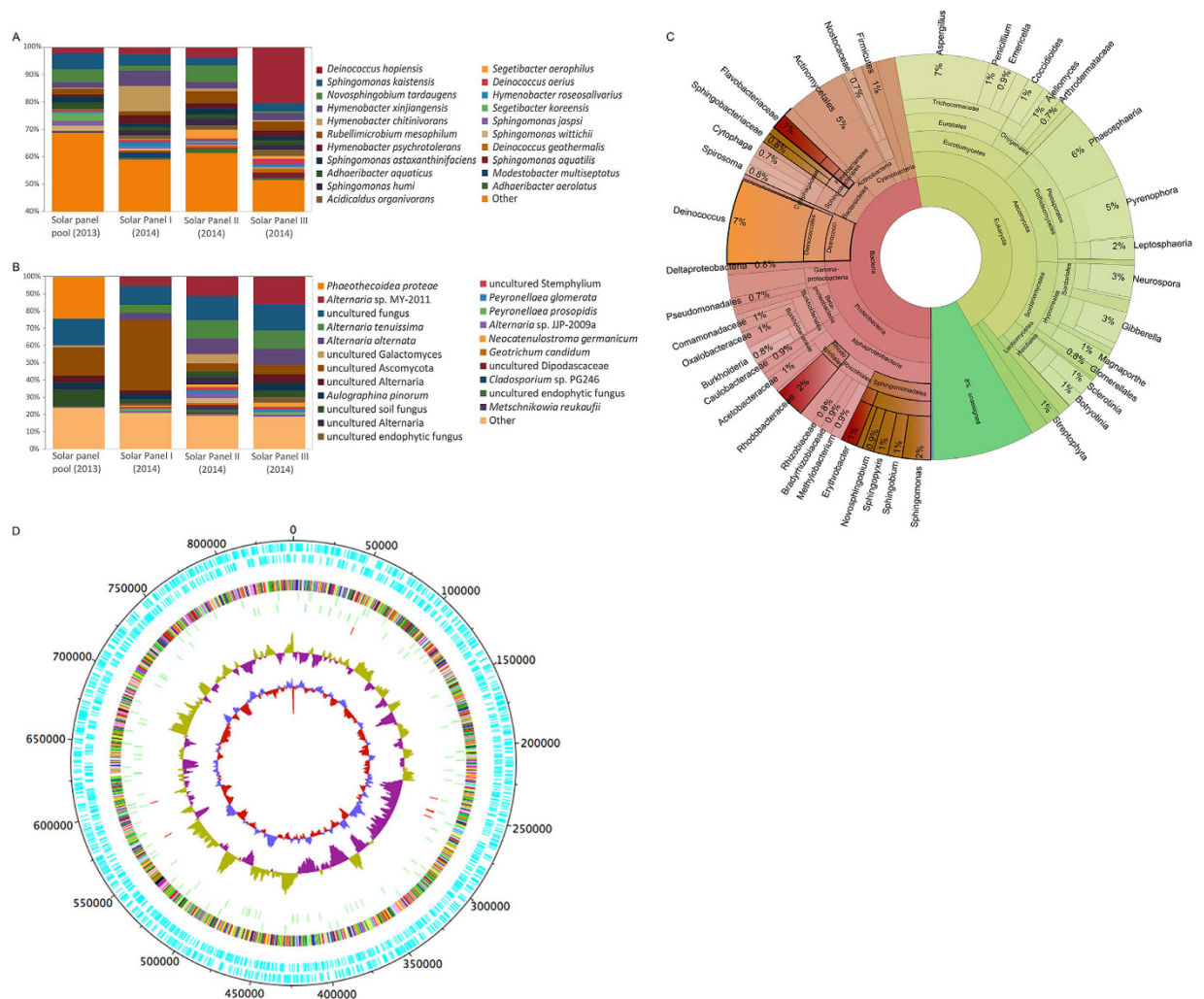


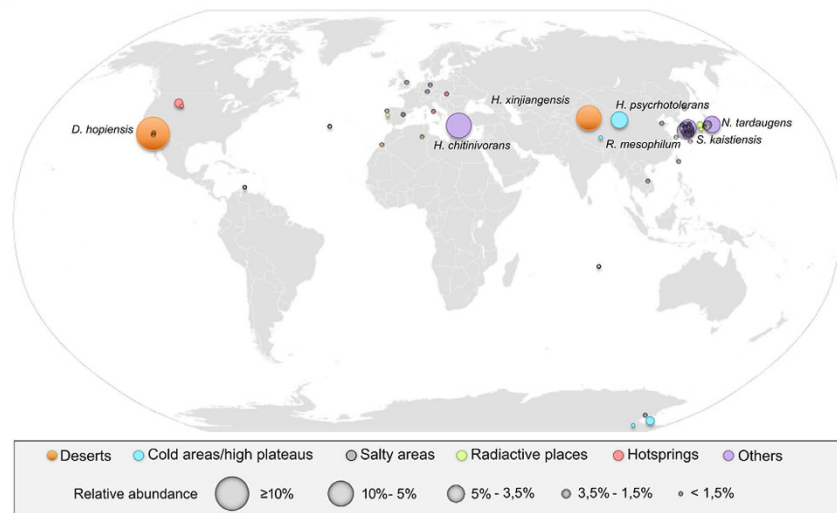
Figure 1. Taxonomic diversity of solar-panel biocenosis, deduced by culture-independent techniques.

Diversity of bacteria (A) and fungi (B) analyzed by 16S and 18S rRNA gene sequencing, respectively, of solar panels sampled during the Summer solstice of 2013 (pool of samples) and 2014 (three solar panels independently analyzed). Histograms show the relative abundance (%) of the species identified, as described in Methods. Species representing less than 1% of total reads were clustered and labeled as “Other”. Taxonomic diversity of one of the panels (panel 3) sampled in the summer solstice of 2014 as deduced from shotgun metagenomic sequencing (C). Carotenoid and sphingolipid-producing bacteria are highlighted in red and brown, respectively. Radiation-resistant phyla are highlighted in orange. The taxonomic diversity of solar panel 1 is represented in Figure S3. Circular representation of the *Deinococcus* solar panel pangenome (D) obtained from the metagenomic sequences of panels 1 and 3. The map includes (from the outer to the inner circle) the ORFs in forward and reverse sense, a colour-coded COG functional annotation, the predicted tRNAs and rRNAs, the GC count, and the GC skew.

most of the species identified by high throughput sequencing, and particularly the most frequent ones, are known to produce pink (*H. xingiangensis*¹⁹, *H. psychrotolerans*²⁰), orange (*Sphingomonas humi*²¹), orange-red (*S. kaistensis*²²) or reddish pigments (*Hymenobacter chitinivorans*²³, *Rubellimicrobium mesophilum*²⁴), in most cases carotenoids; as well as sphingolipids (*Sphingomonas* spp.^{21,22}, *Novosphingobium* spp.²⁵). Carotenoids have been reported to play a major role in radiation tolerance in bacteria²⁶ and sphingolipids have recently been described to mediate bacteria-to-silica and –polyamide adhesion²⁷. Therefore, carotenoids and sphingolipids are candidates accounting for the sunlight resistance and fixation properties that microorganisms need to survive on a smooth, south-facing surface.

A review of the ecology of the main bacterial taxa we identified gives more insights of the extremophile character of the solar panel bacteriome. Indeed, several of the most frequent *Deinococcus* spp. and other solar-panel bacteria have been described as inhabitants of relatively mild desertic areas as well as polar environments. *D. hopiensis* was isolated from the Sonora desert²⁸, while other *Deinococcus* species that we detected were first described in the Sahara desert²⁹. Regarding other very abundant species, such as *Hymenobacter xingiangensis* or *Sphingomonas kaistensis*, they have previously been reported on the high Tibet plateau²⁰, on dry Antarctic valleys³⁰, or in the Chinese desert of Xingiang¹⁹. Others were first reported in high salinity areas³¹, thermal springs³²

A



B

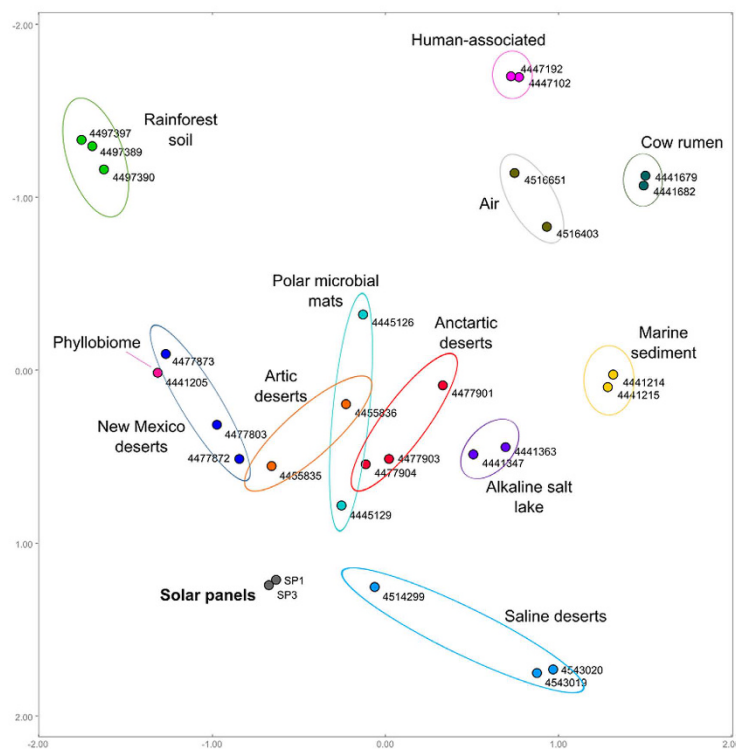


Figure 3. Biogeographical context of the solar-panel microbiomes as deduced from their taxonomic profile. Geographic distribution (A) of the 50 most abundant (more than 1% of the reads) bacterial species detected by high-throughput sequencing of 16S rRNA amplicons in solar panels sampled at the University of Valencia in 2014. Each circle corresponds to a different species and the size of the circles is proportional to the number of reads. Species found at a frequency higher than 3.5% are shown. Colors indicate type of environment. The world map (<https://commons.wikimedia.org/wiki/File:BlankMap-World6.svg>) is licensed under the Creative Commons Public Domain license. The license terms can be found on the following link: <https://creativecommons.org/publicdomain/mark/1.0/>. Principal Coordinates Analysis (B) performed with the taxonomic profile of a range of metagenomes from diverse ecosystems. The solar-panel metagenomes (panels 1 and 3 from the 2014 sampling, grey dots) map within desert and circumpolar metagenomes.

cultures. Microbial interactions (including pH and salinity tolerance restoration), physical effects such as shading, DNA repair mechanisms and production of pigments and adhesion molecules might play a major role in the adaptation of a unique microbial ecosystem to the abrupt circadian cycles in desert-like conditions. This previously undescribed ecosystem is the first urban microdesert reported to date, and it may provide a valuable new source of compounds with biotechnological applications.

Methods

Sampling. Sampling was performed during the summer solstice of 2013 and 2014. Sampling consisted of a simple harvesting procedure, by pouring sterile PBS (sodium phosphate buffer) on the panel and immediately harvesting the liquid by strongly and repeatedly scraping the surface with a modified window cleaner with an autoclaved silicone tube measuring 5 mm in diameter. The resulting suspension was collected by using a sterile plastic pipette and transferred to sterile Falcon tubes, placed on ice and immediately transported to the lab. Solar panels had a surface of 1.28 m², had been in operation for at least 5 years, and the different panels sampled were separated at least 10 meters to avoid statistical biases in microbial composition. In 2013, nine samples from solar panels on the three campuses of the University of Valencia (Valencia, Spain) were collected at noon (2 PM) and pooled together for further analysis through 16S/18S rRNA sequencing and cultivation methods. Air temperature was 33 °C and relative humidity was 60%. In 2014, we sampled three solar panels from a single location (Faculty of Economics, University of Valencia, Valencia, Spain) under day (2 PM) and night conditions (4 AM). Day-collected samples were independently analyzed through 16S/18S rRNA sequencing, Illumina shotgun sequencing (only two of the panels sampled), and metaproteomics; whereas night-collected samples were only used for the metaproteomic analysis. Air temperature and relative humidity were 32 °C and 56% (2 PM), and 23 °C and 83% (4 AM).

The average temperature of the panels' surface during the sampling process (at 2 PM) was 51 °C. The average solar irradiance in Valencia at 2 PM is 461.3 W/m², whereas the accumulated solar irradiance during an average day is 19.6 kJ/m². According to the reports of AEMET (Spanish State Meteorological Agency), the weather conditions in Valencia were similar between May-June 2013 and May-June 2014 (the periods prior to summer solstice when sampling took place). In 2013, the temperature of the one-month period prior sampling was 0.8 °C lower than the average, and the precipitation levels dropped a 20% with respect to the last decade. In contrast, in 2014, the temperature of the one-month period prior sampling was 0.5 °C higher than the average, and normal precipitation levels were recorded. The microbial profiles displayed no major changes between 2013 and 2014.

Microbiological media and growth conditions. Three culture media (LB medium, R2A medium, and marine agar) were used in this work according to our previous experience in other highly irradiated environments, where those media proved optimal to detect pigment-producing strains. Aliquots of 100 µL from the solar-panel samples were spread on Petri dishes containing LB medium (composition in g/L: peptone 10.0, NaCl 10.0, yeast extract 5.0), R2A medium (composition in g/L: peptone 0.5, casaminoacids 0.5, yeast extract 0.5, dextrose 0.5, soluble starch 0.5, K₂HPO₄ 0.3, MgSO₄ 0.05, sodium pyruvate 0.3) or marine medium (composition in g/L: peptone 5.0, yeast extract 1.0, ferric citrate 0.1, NaCl 19.45, MgCl₂ 5.9, Na₂SO₄ 3.24, CaCl₂ 1.8, KCl 0.55, NaHCO₃ 0.16, KBr 0.08, SrCl₂ 0.034, H₃BO₃ 0.022, Na₄O₄Si 0.004, NaF 0.024, NH₄NO₃ 0.0016, Na₂HPO₄ 0.008), and incubated at room temperature (previous tests were performed at different temperatures, but the largest number of colonies was observed at room temperature) for 7 days. Individual colonies were independently re-streaked on new media and pure cultures were finally identified through 16S rRNA sequencing and cryo-preserved in 20% glycerol (v/v) until required. A total of 53 bacterial strains were characterized under stress conditions and serially confronted with each other in solid medium to detect interactions in terms of resistance to harsh conditions.

Strains stress tests. Each strain was subjected to a range of stress assays to test tolerance to salinity, heat, low pH, and UV radiation. Overnight liquid cultures were adjusted to an OD₆₀₀ value of 0.03. Then, stress tests were carried out by plating several 20 µL droplets of the diluted culture on LB, R2A, or marine agar with the following modifications. In the case of salinity stress, increasing amounts of NaCl (from 1 to 9% w/v) were added to the media (final concentration ranging from 1 to 26% w/v). To test pH resistance, culture media was adjusted to pH 5, 6, and 8. In the case of heat, plates were incubated overnight at 60 °C; whereas resistance to radiation was tested by applying UV pulses of different length (30 s, 2 min, and 8 min) with a VL-4C lamp (254 nm, 340 µW cm⁻²; Labolan, S.L., Spain). The XL1-Blue *E. coli* strain was used as control. For each experiment, two independent replicates were performed.

In order to detect inhibition or synergistic effects between strains, experiments were performed as described above and strain suspensions (20 µL) were closely (3 mm) placed on the same dish.

DNA isolation. Selected DNA purification methods were used to process the solar panels samples and DNA yields were compared (data not shown). Metagenomic DNA was isolated using the Power Soil DNA Isolation kit (MO BIO Laboratories) following the manufacturer's instructions with an additional pretreatment with DNA-free lysozyme at 37 °C for 10 min. The quantity and quality of the DNA was determined on a 1.5% agarose gel and with a Nanodrop-1000 Spectrophotometer (Thermo Scientific, Wilmington, DE).

PCR amplification and 16S/18S rRNA massive sequencing. A set of primers adapted to massive sequencing for the Ion Torrent platform (Life technologies) were used to capture 16S (modified from a previous study⁴²) and 18S (modified from a previous study⁴³) rRNA from the solar-panel DNA extraction in a PCR reaction. PCR reactions were performed with 30 ng of metagenomic DNA, 200 µM of each of the four deoxynucleoside triphosphates, 400 nM of each primer, 2.5 U of FastStart HiFi Polymerase, and the appropriate buffer with MgCl₂ supplied by the manufacturer (Roche, Mannheim, Germany), 4% of 20 g/mL BSA (Sigma, Dorset, United Kingdom), and 0.5 M Betaine (Sigma). Thermal cycling consisted of initial denaturation at 94 °C for 2 minutes followed by 35 cycles of denaturation at 94 °C for 20 seconds, annealing at 50 °C for 30 seconds, and extension at 72 °C for 5 minutes.

Amplicons were combined in a single tube in equimolar concentrations. The pooled amplicon mixture was purified twice (AMPure XP kit, Agencourt, Takeley, United Kingdom) and the cleaned pool requantified using

the PicoGreen assay (Quant-iT, PicoGreen DNA assay, Invitrogen). Subsequently, sequencing on the Ion Torrent platform was performed at LifeSequencing S.L. (Valencia, Spain).

Shotgun metagenomic sequencing. The metagenomic DNA of two of the solar panels sampled in 2014 (solar panels 1 and 3, from which enough DNA was available) was shotgun sequenced. A Nextera Illumina library was built from 100 ng total DNA following the protocol indications marked by Illumina. Those libraries were sequenced in a MiSeq sequencer (Illumina) at Lifesequencing SL, in a combination of 500 cycles, in order to obtain 250 bp paired-end sequences.

Bioinformatic analysis. *16S/18S rRNA profiles.* The resulting sequences from the taxonomical identification, based on PCR capturing of the 16S and 18S rRNA, were split taking into account the barcode introduced during the PCR reaction, providing a single FASTQ file for each of the samples. We performed quality filtering (Q20) using fastx tool kit version 0.013, primer (16S and 18S rRNA primers) trimming using cutadapt version 1.4.1 and length (minimum 300 bp read length) trimming using in-house perl scripting over those FASTQ files to obtain a FASTQ file with clean data. Those clean FASTQ files were converted to FASTA files and UCHIME⁴⁴ program version 7.0.1001 was used to remove chimeras arising during the amplification and sequencing step.

Those clean FASTA files were BLAST against NCBI 16S rRNA and fungi database using blastn version 2.2.29+. The resulting XML file were processed using a pipeline developed by Lifesequencing S.L. (Paterna, Valencia, Spain) in order to annotate each sequence at different phylogenetic levels (Phylum, Family, Genera and Species). Statistical analysis was performed using R version 3.1.1. A summary of sequencing statistics and results is available in Table S2.

Taxonomic and functional analysis of metagenomic sequences. Two FASTQ files per sample were obtained during the sequencing step, each coming from each of the directions on the paired-end sequencing. Those files were trimmed for adapters and low quality reads using cutadapt version 1.4.1 with the paired-end option. Trimmed sequences were used for taxonomical identification using a local alignment tool against nt database from NCBI as described before⁴⁵. The trimmed sequences from each solar panel were also assembled using different combinations of k-mers in Abyss version 1.5.2⁴⁶ and Velvet version 1.2.1⁴⁷ in order to find the best combination. The best assembly in each solar panel was used to perform a prediction of ORFs by using MetaGeneMark⁴⁸. BLASTP against nr NCBI database was used for annotation and webMGA⁴⁹ for COG assignment. All our data have been deposited in the MG-RAST server, and is publicly available under accession numbers 4629146.3 and 4629747.3.

In order to compare the taxonomic profile of solar panels with other environments, the taxonomic information of 25 metagenomes belonging to different habitats was obtained from the MG-RAST server (IDs 4455835.3, 4455836.3, 4477803.3, 4477872.3, 4477873.3, 4441205.3, 4445129.3, 4445126.3, 4477903.3, 4477904.3, 4477901.3, 4514299.3, 4543019.3, 4543020.3, 4441347.3, 4441363.3, 4441215.3, 4441214.3, 4441679.3, 4441682.3, 4447192.3, 4447102.3, 4497390.3, 4497389.3, 4497397.3, 4516651.3, and 4516403.3). The different profiles were processed with MEGAN. Data were normalized, and the distances between pairs of profiles calculated with the Bray-Curtis method. Finally, the calculated distances were used to build a Principal Coordinates Analysis. We employed the Statistical Analysis of Metagenomic Profiles (STAMP) (version 1.08; Faculty of Computer Science, Dalhousie University) software to compare the functional profile (according to subsystems categories) of our samples with those of the metagenomes previously cited. The functional data of metagenomes 4455835.3, 4455836.3, 4477803.3, 4477872.3, 4477873.3, 4477903.3, 4477904.3, 4477901.3, 4514299.3 was poor or absent, and was thus eliminated from the analysis. This comparison was represented in a heatmap, where the different metagenomes are clustered according to their similarity. The functional contents of solar panels 1 and 3 were compared to each other with a Fisher's exact test combined with the Newcombe-Wilson method for calculating confidence intervals (nominal coverage of 95%). As a multiple-hypothesis test correction, a false-discovery-rate (FDR) method was applied.

Pangenome reconstruction. Trimmed sequences from both solar panels for the total DNA experiment were blasted against a database containing all sequences for the genera Thermo/Deinococcus. Only sequences with a positive hit in against this database were used for assembly them using different k-mers with the Abyss assembler. We performed a genome annotation in different steps i) ORFs were predicted with GeneMark version 3.25⁴⁸, ii) rRNA version 1.2⁵⁰ for rRNA prediction, and iii) tRNA-Scan⁵¹ for tRNA prediction. The functional annotation using COG classification was performed using webMGA. DNAPlotter⁵² from the Artemis Package was used to represent a circular map of the pangenome.

Proteomics. Protein samples were precipitated with TCA (trichloroacetic acid) and pellets were dissolved with 75 μ L of 50 mM ABC (ammonium bicarbonate). The protein concentration in the samples was determined by fluorometric analysis. Then, 10 μ g of each sample were digested as described in the following protocol. Cysteine residues were reduced by 2 mM DTT (DL-Dithiothreitol) in 50 mM ABC at 60 °C for 20 min. Sulfhydryl groups were alkylated with 5 mM IAM (iodoacetamide) in 50 mM ABC in the dark at room temperature for 30 min. IAM excess was neutralized with 10 mM DTT in 50 mM ABC, 30 min at room temperature. Each sample was subjected to trypsin digestion with 250 ng (100 ng/ μ L) of sequencing grade modified trypsin (Promega) in 50 mM ABC at 37 °C overnight. The reaction was stopped with TFA (trifluoroacetic acid) at a final concentration of 0.1%. Final peptide mixture was concentrated in a speed vacuum and resuspended in 30 μ L of 2% ACN, 0.1% TFA. Finally, 5 μ L of each sample were loaded onto a trap column (NanoLC Column, 3 μ C18-CL, 75 μ m \times 15 cm; Eksigen) and desalted with 0.1% TFA at 2 μ L/min during 10 min.

The peptides were then loaded onto an analytical column (LC Column, 3 μ C18-CL, 75 μ m \times 25 cm, Eksigen) equilibrated in 5% acetonitrile 0.1% FA (formic acid). Elution was carried out with a linear gradient of 5:35% B

in A for 40 min (A: 0.1% FA; B: ACN, 0.1% FA) at a flow rate of 300 nl/min in a label free mode. Peptides were analyzed in a mass spectrometer nanoESI qTOF (5600 TripleTOF, ABSCIEX). The tripleTOF was operated in information-dependent acquisition mode, in which a 0.25-s TOF MS scan from 350–1250 m/z, was performed, followed by 0.05-s product ion scans from 100–1500 m/z on the 25 most intense 2–5 charged ions.

ProteinPilot default parameters were used to generate a peak list directly from 5600 TripleTof wiff files. The Paragon algorithm of ProteinPilot was used to search NCBI protein database with the following parameters: trypsin specificity, cys-alkylation, no taxonomy restriction, and the search effort set to through. To avoid using the same spectral evidence in more than one protein, the identified proteins were grouped based on MS/MS spectra by the Protein-Pilot Progroup algorithm. The PeakView v 1.1 (ABSciex) software was used to generate the peptides areas from Protein Pilot result files and to perform a principal component (PCA) and a t-test analysis.

References

1. Corliss, J. B. *et al.* Submarine thermal springs on the galapagos rift. *Science* **203**, 1073–1083 (1979).
2. Singh, A. & Lal, R. *Sphingobium ummariense* sp. nov., a hexachlorocyclohexane (HCH)-degrading bacterium, isolated from HCH-contaminated soil. *Int. J. Syst. Evol. Microbiol.* **59**, 162–166 (2009).
3. Neilson, J. W. *et al.* Life at the hyperarid margin: novel bacterial diversity in arid soils of the Atacama Desert, Chile. *Extremophiles* **16**, 553–566 (2012).
4. Rosche, B., Li, X. Z., Hauer, B., Schmid, A. & Buehler, K. Microbial biofilms: a concept for industrial catalysis? *Trends Biotechnol.* **27**, 636–643 (2009).
5. Williamson, A. J. *et al.* Microbial reduction of U(VI) under alkaline conditions: implications for radioactive waste geodisposal. *Environ. Sci. Technol.* **48**, 13549–13556 (2014).
6. Pham, N. T. A. & Anonye, B. O. Vying over spilled oil. *Nat. Rev. Microbiol.* **12**, 156 (2014).
7. Martin, L. J. *et al.* Evolution of the indoor biome. *Trends Ecol. Evol.* **30**, 223–232 (2015).
8. Adams, R. I., Bateman, A. C., Bik, H. M. & Meadow, J. F. Microbiota of the indoor environment: a meta-analysis. *Microbiome* **3**, 49 (2015).
9. Mahnert, A., Moissl-Eichinger, C. & Berg, G. Microbiome interplay: plants alter microbial abundance and diversity within the built environment. *Front. Microbiol.* **6**, 887 (2015).
10. Robertson, C. E. *et al.* Culture-independent analysis of aerosol microbiology in a metropolitan subway system. *Appl. Environ. Microbiol.* **79**, 3485–3493 (2013).
11. Leung, M. H. Y., Wilkins, D., Li, E. K. T., Kong, F. K. F. & Lee, P. K. H. Indoor-air microbiome in an urban subway network: diversity and dynamics. *Appl. Environ. Microbiol.* **80**, 6760–6770 (2014).
12. Afshinnekoo, E. *et al.* Geospatial Resolution of Human and Bacterial Diversity with City-Scale Metagenomics. *Cell Syst.* **1**, 72–87 (2015).
13. Römling, U., Galperin, M. Y. & Gomelsky, M. Cyclic di-GMP: the first 25 years of a universal bacterial second messenger. *Microbiol. Mol. Biol. Rev.* **77**, 1–52 (2013).
14. Diaconu, M. *et al.* Structural basis for the function of the ribosomal L7/12 stalk in factor binding and GTPase activation. *Cell* **121**, 991–1004 (2005).
15. Baykov, A. A., Malinen, A. M., Luoto, H. H. & Lahti, R. Pyrophosphate-fueled Na⁺ and H⁺ transport in prokaryotes. *Microbiol. Mol. Biol. Rev.* **77**, 267–276 (2013).
16. Etchegaray, J. P. & Inouye, M. CspA, CspB, and CspG, major cold shock proteins of *Escherichia coli*, are induced at low temperature under conditions that completely block protein synthesis. *J. Bacteriol.* **181**, 1827–1830 (1999).
17. Cascales, E., Bernadac, A., Gavioli, M., Lazzaroni, J.-C. & Lloubes, R. Pal Lipoprotein of *Escherichia coli* Plays a Major Role in Outer Membrane Integrity. *J. Bacteriol.* **184**, 754–759 (2002).
18. Rothfuss, H. Involvement of the S-layer proteins Hpi and SlpA in the maintenance of cell envelope integrity in *Deinococcus radiodurans* R1. *Microbiology* **152**, 2779–2787 (2006).
19. Zhang, Q. *et al.* *Hymenobacter xinjiangensis* sp. nov., a radiation-resistant bacterium isolated from the desert of Xinjiang, China. *Int. J. Syst. Evol. Microbiol.* **57**, 1752–1756 (2007).
20. Zhang, G. *et al.* *Hymenobacter psychrotolerans* sp. nov., isolated from the Qinghai–Tibet Plateau permafrost region. *Int. J. Syst. Evol. Microbiol.* **58**, 1215–1220 (2008).
21. Yi, T. H., Han, C.-K., Srinivasan, S., Lee, K. J. & Kim, M. K. *Sphingomonas humi* sp. nov., isolated from soil. *J. Microbiol.* **48**, 165–169 (2010).
22. Kim, M. K. *et al.* *Sphingomonas kaistensis* sp. nov., a novel alphaproteobacterium containing pufLM genes. *Int. J. Syst. Evol. Microbiol.* **57**, 1527–1534 (2007).
23. Buczolits, S., Denner, E. B. M., Kämpfer, P. & Busse, H.-J. Proposal of *Hymenobacter norwichensis* sp. nov., classification of ‘*Taxeobacter ocellatus*’, ‘*Taxeobacter gelipurpurascens*’ and ‘*Taxeobacter chitinovorans*’ as *Hymenobacter ocellatus* sp. nov., *Hymenobacter gelipurpurascens* sp. nov. and *Hymenobacter chitinivo*. *Int. J. Syst. Evol. Microbiol.* **56**, 2071–2078 (2006).
24. Dastager, S. G., Lee, J.-C., Ju, Y.-J., Park, D.-J. & Kim, C.-J. *Rubellimicrobium mesophilum* sp. nov., a mesophilic, pigmented bacterium isolated from soil. *Int. J. Syst. Evol. Microbiol.* **58**, 1797–1800 (2008).
25. Fujii, K. *et al.* *Novosphingobium tardaagens* sp. nov., an oestradiol-degrading bacterium isolated from activated sludge of a sewage treatment plant in Tokyo. *Int. J. Syst. Evol. Microbiol.* **53**, 47–52 (2003).
26. Tian, B. & Hua, Y. Carotenoid biosynthesis in extremophilic *Deinococcus*-*Thermus* bacteria. *Trends Microbiol.* **18**, 512–520 (2010).
27. Gutman, J. *et al.* Interactions of glycosphingolipids and lipopolysaccharides with silica and polyamide surfaces: adsorption and viscoelastic properties. *Biomacromolecules* **15**, 2128–2137 (2014).
28. Rainey, F. A. *et al.* Extensive diversity of ionizing-radiation-resistant bacteria recovered from Sonoran Desert soil and description of nine new species of the genus *Deinococcus* obtained from a single soil sample. *Appl. Environ. Microbiol.* **71**, 5225–5235 (2005).
29. de Groot, A. *et al.* *Deinococcus deserti* sp. nov., a gamma-radiation-tolerant bacterium isolated from the Sahara Desert. *Int. J. Syst. Evol. Microbiol.* **55**, 2441–2446 (2005).
30. Hirsch, P. *et al.* *Hymenobacter roseosalivarius* gen. nov., sp. nov. from continental Antarctica soils and sandstone: bacteria of the *Cytophaga/Flavobacterium/Bacteroides* line of phylogenetic descent. *Syst. Appl. Microbiol.* **21**, 374–383 (1998).
31. Nübel, U., Garcia-Pichel, F. & Muyzer, G. The halotolerance and phylogeny of cyanobacteria with tightly coiled trichomes (*Spirulina* Turpin) and the description of *Halospirulina tapeticola* gen. nov., sp. nov. *Int. J. Syst. Evol. Microbiol.* **50** Pt 3, 1265–1277 (2000).
32. Alarico, S. *et al.* *Rubritepida flocculans* gen. nov., sp. nov., a new slightly thermophilic member of the alpha-1 subclass of the Proteobacteria. *Syst. Appl. Microbiol.* **25**, 198–206 (2002).
33. Yoon, J.-H., Kang, S.-J., Lee, S.-Y. & Oh, T.-K. *Sphingomonas insulae* sp. nov., isolated from soil. *Int. J. Syst. Evol. Microbiol.* **58**, 231–236 (2008).
34. Pradhan, S. *et al.* Bacterial biodiversity from Roopkund Glacier, Himalayan mountain ranges, India. *Extremophiles* **14**, 377–395 (2010).
35. Yang, Y. *et al.* *Deinococcus aeriis* sp. nov., isolated from the high atmosphere. *Int. J. Syst. Evol. Microbiol.* **59**, 1862–1866 (2009).
36. Yoo, S.-H. *et al.* *Roseomonas aerilata* sp. nov., isolated from an air sample. *Int. J. Syst. Evol. Microbiol.* **58**, 1482–1485 (2008).

37. Crous, P. W., Summerell, B. A., Mostert, L. & Groenewald, J. Z. Host specificity and speciation of *Mycosphaerella* and *Teratosphaeria* species associated with leaf spots of Proteaceae. *Persoonia* **20**, 59–86 (2008).
38. Sláviková, E., Vadkertiová, R. & Vránová, D. Yeasts colonizing the leaf surfaces. *J. Basic Microbiol.* **47**, 344–350 (2007).
39. Zakharova, K. *et al.* Microcolonial fungi on rocks: a life in constant drought? *Mycopathologia* **175**, 537–547 (2013).
40. Rosselli, R. *et al.* Microbial immigration across the Mediterranean via airborne dust. *Sci. Rep.* **5**, 16306 (2015).
41. Shirakawa, M. A. *et al.* Microbial colonization affects the efficiency of photovoltaic panels in a tropical environment. *J. Environ. Manage.* **157**, 160–167 (2015).
42. Sim, K. *et al.* Improved detection of bifidobacteria with optimised 16S rRNA-gene based pyrosequencing. *PLoS One* **7**, e32543, doi: 10.1371/journal.pone.0032543 (2012).
43. La Duc, M. T., Vaishampayan, P., Nilsson, H. R., Torok, T. & Venkateswaran, K. Pyrosequencing-derived bacterial, archaeal, and fungal diversity of spacecraft hardware destined for Mars. *Appl. Environ. Microbiol.* **78**, 5912–5922 (2012).
44. Edgar, R. C., Haas, B. J., Clemente, J. C., Quince, C. & Knight, R. UCHIME improves sensitivity and speed of chimera detection. *Bioinformatics* **27**, 2194–2200 (2011).
45. Ames, S. K. *et al.* Using populations of human and microbial genomes for organism detection in metagenomes. *Genome Res.* **25**, 1056–1067 (2015).
46. Simpson, J. T. *et al.* ABySS: a parallel assembler for short read sequence data. *Genome Res.* **19**, 1117–1123 (2009).
47. Zerbino, D. R. & Birney, E. Velvet: algorithms for de novo short read assembly using de Bruijn graphs. *Genome Res.* **18**, 821–829 (2008).
48. Besemer, J., Lomsadze, A. & Borodovsky, M. GeneMarkS: a self-training method for prediction of gene starts in microbial genomes. Implications for finding sequence motifs in regulatory regions. *Nucleic Acids Res.* **29**, 2607–2618 (2001).
49. Wu, S., Zhu, Z., Fu, L., Niu, B. & Li, W. WebMGA: a customizable web server for fast metagenomic sequence analysis. *BMC Genomics* **12**, 444 (2011).
50. Lagesen, K. *et al.* RNAmmer: consistent and rapid annotation of ribosomal RNA genes. *Nucleic Acids Res.* **35**, 3100–3108 (2007).
51. Lowe, T. M. & Eddy, S. R. tRNAscan-SE: a program for improved detection of transfer RNA genes in genomic sequence. *Nucleic Acids Res.* **25**, 955–964 (1997).
52. Carver, T., Thomson, N., Bleasby, A., Berriman, M. & Parkhill, J. DNAPlotter: circular and linear interactive genome visualization. *Bioinformatics* **25**, 119–120 (2009).

Acknowledgements

The authors are indebted to the Vicerrectorat d'Infraestructures (University of Valencia) for their support before and during sampling. Biopolis SL funded this work. C.V. is a recipient of a FPU (Formación de Personal Universitario) grant from the Spanish MEC (Ministerio de Educación, Cultura y Deporte). We also thank the proteomics service (SCSIE) of the University of Valencia for its technical support and Fabiola Barraclough for English revision.

Author Contributions

M.P., D.R. and J.P. designed the experiments. P.D.-M. and C.V. performed the experiments. F.M.C. and C.V. performed the bioinformatic analysis. P.D.-M., M.P., J.P., D.R. and C.V. analyzed the data. P.D. and C.V. contributed equally to this work. All authors wrote and revised the manuscript.

Additional Information

Supplementary information accompanies this paper at <http://www.nature.com/srep>

Competing financial interests: The authors declare no competing financial interests.

How to cite this article: Dorado-Morales, P. *et al.* A highly diverse, desert-like microbial biocenosis on solar panels in a Mediterranean city. *Sci. Rep.* **6**, 29235; doi: 10.1038/srep29235 (2016).



This work is licensed under a Creative Commons Attribution 4.0 International License. The images or other third party material in this article are included in the article's Creative Commons license, unless indicated otherwise in the credit line; if the material is not included under the Creative Commons license, users will need to obtain permission from the license holder to reproduce the material. To view a copy of this license, visit <http://creativecommons.org/licenses/by/4.0/>